PREDICTING ESTUARINE CHLOROPHYLL A SPATIAL DISTRIBUTION AT EBB AND FLOOD TIDE FROM AIRBORNE MULTISPECTRAL SCANNER DATA

by

GLENN PAUL CATTS

A Thesis Submitted to
the Graduate Faculty of
North Carolina State University
in Partial Fulfillment of the Requirements
for the Degree of Master of Science

Department of Forestry

Raleigh

1984

APPROVED:

James D. Gregory William L. Hafley

Samuel Burgan
Chairman, Advisory Committee

ABSTRACT

CATTS, GLENN PAUL. Predicting Estuarine Chlorophyll *a* Spatial Distribution at Ebb Tide and Flood Tide from Airborne Multispectral Scanner Data. (Under the direction of SIAMAK KHORRAM.)

Simultaneous acquisition of surface chlorophyll *a* concentrations for 39 samples from boats and radiance measurements in the visible and near infra-red wavelengths of the electro-magnetic spectrum made by a Daedalus 1260 Multispectral Scanner data from a U-2 aircraft was conducted in the northern reaches of San Francisco Bay on August 28, 1980. These data were used to develop regression models for predicting surface chlorophyll *a* concentrations over the study area for ebb tide (8:40 A.M. PDT) and flood tide (3:10 P.M. PDT) conditions. After selection of a single "best fitting" model for both morning and afternoon data sets, chlorophyll *a* concentration was predicted for ebb and flood tide for the entire study area at approximately 40 m x 40 m resolution. The predicted spatial display of chlorophyll *a* revealed a localized area of high phytoplankton biomass that has been inferred from field surveys and appears to be a common summer phenomenon.

Knowledge of the distribution of phytoplankton and the location of this zone of high biomass is valuable in establishing management policies for this ecologically

important estuary. Furthermore, the techniques used here may provide an alternative cost-effective method for assessing water quality conditions and they may prove useful for studying spatial variations (patchiness) and seasonal variations in phytoplankton biomass in other estuaries and coastal waters.

BIOGRAPHY

Glenn Paul Catts was born in Wilmington, Delaware, on February 25, 1956. Before graduating from Christiana High School in Newark, Delaware, in 1974, he lived in Berkeley, California (5 years) and Pullman, Washington (1/2 year). He attended the University of Delaware and graduated in 1978 with a Bachelor of Arts and Science degree in a double major curriculum of Physical Anthropology and Physical Geography.

In August, 1979, he entered Louisiana State University where he spent one academic year of residence pursuing a Master of Science degree in Climatology. Introduced to the technology of remote sensing at this time, he left LSU and followed Dr. Siamak Khorram to North Carolina State University where he began a Master of Science degree program in Forestry in the fall of 1981.

Glenn Catts is currently single with avid interests including stained glass, photography, and all outdoor activities.

ACKNOWLEDGEMENTS

The ability to harness one's mental energy toward the goal of attaining better understanding of basic physical and biological processes, with every intent to benefit mankind, is a trying, frustrating and rewarding exercise. I have actually enjoyed racking my brain over problems which seemed insignificant at times.

The realization that nothing is insignificant and that all parts must blend to a cooperative whole I must attribute to my close contact with Dr. Siamak Khorram. I salute his patience with my naivete and youth and have truly appreciated his and Raquel's kindness and generosity. They showed interest in me as a human being, not just a career-hungry grad student. I was very lucky to have them both as advisors.

I would also like to recognize committee members, Dr. Jim Gregory, Dr. William Hafley, and the late Dr. Tom Gemmer for giving me a forestry education the best they know how. I appreciate their dedication, explanations, and assistance in my academic career.

The staff of the Remote Sensing Research Program at the University of California-Berkeley is a wonderful bunch and y'all make the summer research transition fun. My work efficiency was higher because of you. Thanks.

Dr. Jim Cloern deserves my special thanks. He routed me back to the biology wherein some of the basic answers controlling the future of remote sensing of water quality are found. I consider you my "California advisor." In the same breath, thanks to Dr. R. N. Colwell for lending support and advice to both Dr. Khorram and myself. I thoroughly enjoyed meeting you and learning your legacy--you'll always be the inspiration for many young RSM (Remote Sensing Men).

To Betty and Kim, the two whose digits danced my manuscripts into "fact"; two big kisses on your lips--or handshakes if you prefer. Without you both no one would ever read this. Gracias.

Finally, thanks to my friends--and you know who you are: Mom, Dad, Wade, Paul, Vince, Hopps, Coop, Harp, Peeno, Ramon, Dave, Wally, et al. Your support throughout life is much more of a reward than any academic degree.

And when things were the worst, thanks to Sheryl Diane Brown for putting up with me.

This work is a result of research sponsored in part by NOAA, National Sea Grant College Program Department of Commerce, under Grant Number NA80AA-D-00120, Project Number R1CZ-68, through the California Sea Grant College Program, and in part by the California State Resources Agency. The U.S. Government is authorized to reproduce and distribute for governmental purposes.

TABLE OF CONTENTS

LIST OF TABLES

LIST OF FIGURES

Figure No. Page

INTRODUCTION

The northern reach of San Francisco Bay is the closest portion of that estuary to fresh water inflow from the Sacramento and San Joaquin rivers. Salinity is constantly changing as tidal influences and freshwater inflow volumes dictate local sources/sinks of nutrients/energy. This region is an important nursery ground for many marine species. A numerical simulation model of estuarine circulation has been developed as a tool for predicting nutrient source/sink areas. Remote sensing based predictions of chlorophyll a concentrations in near surface waters of the estuary are a segment of this simulation model designed to estimate the net advection of phytoplankton biomass from the source regions of the shoals to the sink regions in the channels (Cloern et al., 1983). The goal of San Francisco Bay simulation modeling is to be able to estimate the phytoplankton and zooplankton standing crops and productivity rates in an attempt to estimate their energy input to higher trophic levels; especially juvenile striped bass (Morone saxatilis) production and survival.

Estuaries are dynamic water bodies characterized by temporal changes in water quality that range from short-term (hourly) variations driven primarily by cyclic tidal currents and fluctuating freshwater inflow to long-term (seasonal or inter-annual) variations caused by changes in

meteorological forcings or river discharge. Estuaries are also spatially heterogeneous and often have large horizontal (or vertical) gradients in water properties (e.g., salinity, suspended sediments, phytoplankton biomass) that result from local variations in bathymetry, circulation and mixing, or sources/sinks of dissolved and suspended constituents.

Knowledge of mechanisms that cause spatio-temporal heterogeneity in the water quality of estuaries is based in large part upon the results of *in situ* water sampling that is costly (both in time and money) and often inefficient, particularly if sampling is required over a large geographic area and over more than one time scale. Truly synoptic measurements of water quality from boats are nearly impossible in estuaries having rapid (100 - 200 cm/sec) tidal currents. If specific properties of estuarine waters can be measured accurately using remote sensing techniques, then understanding of mechanisms through which physical processes (tidal advection, estuarine nontidal circulation, horizontal dispersion, and resuspension) effect change in dynamic estuarine waters can be improved.

This general problem is exemplified by the need for better understanding of mechanisms that control phytoplankton dynamics in the northern San Francisco Bay estuary, which has been the focus of intensive field

investigation during the past decade (Conomos, 1979). The upper reach of San Francisco Bay (Suisun Bay, Fig. 1) comprises two deep (~10 - 15 m) channels and a shallow (~ 1 - 2 m) embayment, and is the site of local accumulations of suspended particulates (a turbidity maximum; Conomos and Peterson, 1977) and phytoplankton (a chlorophyll maximum; Peterson et al., 1975) during summer.

The turbidity maximum, a common feature of partially mixed estuaries (Postma, 1967; Meade, 1972), results from two physical processes: particle sinking and estuarine circulation, such that residual (tidally-averaged) surface currents flow seaward while bottom currents flow landward. The result is a trapping mechanism that retains suspended particulates in that region of the estuary (null zone) where the landward bottom current converges with the seaward river current.

These same physical processes apparently also operate on phytoplankton cells (mostly diatoms) in Suisun Bay, and act to retain phytoplankton biomass that is produced over the shoals, where light availability is sufficient to sustain net photosynthesis and growth (Cloern and Cheng, 1981; Cloern et al., 1983). These concepts have evolved from water quality measurements made over a coarse grid of stations that is sampled on weekly time scales or longer. Hence, little is known about small-scale (less than about 2 km) spatial heterogeneity (phytoplankton patchiness,

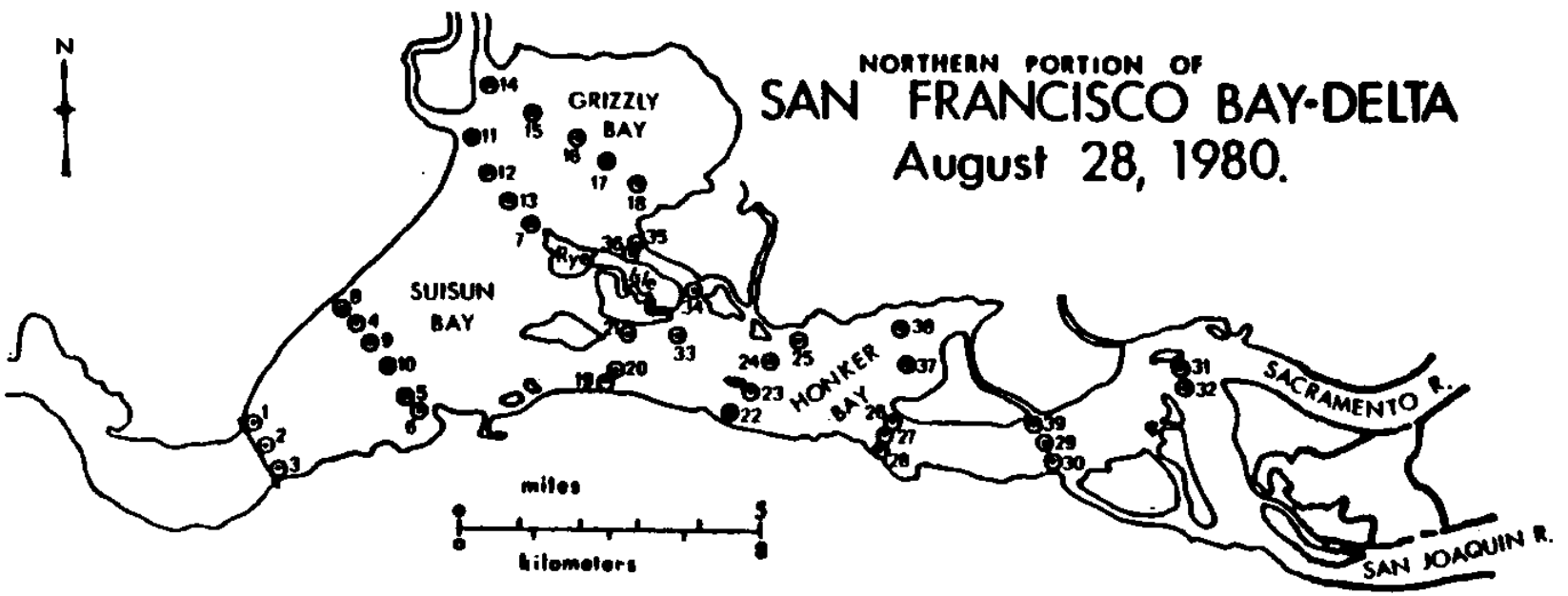

FIGURE 1. The study area and 39 sample site locations.

including that associated with fronts), short-term (hourly or daily) variations in structure of the phytoplankton maximum, or rates of horizontal mixing of water masses between the shoals (the source of phytoplankton biomass) and deeper channels. If remotely-sensed images could accurately represent the horizontal distribution of phytoplankton biomass in turbid shallow waters, then the dynamic nature of the phytoplankton maximum of Suisun Bay and other estuaries may become more clear.

Further, San Francisco Bay, like many urbanized estuaries, is subjected to perturbations (dredging, marsh reclamation, diversions of freshwater inflow, waste discharges) that potentially alter water quality, and remote sensing may be a valuable tool for monitoring the long-term ecological consequences of such perturbations. The purpose of this study is to examine the potential utility of high-resolution multispectral imagery [similar to that provided by the Landsat 4 Thematic Mapper (TM)] for mapping the spatial distribution of phytoplankton biomass (chlorophyll a) in the upper reach of northern San Francisco Bay. Specific objectives were to determine:

(1) whether remotely-sensed reflectance data from a scanner similar to the TM sensor can be used to accurately map surface chlorophyll a concentration in a shallow, turbid environment;

(2) which spectral bands are required for mapping chlorophyll in turbid estuaries;

(3) the mathematical model(s) which most accurately describe chlorophyll concentration; and,

(4) whether mathematical models are conservative over short time scales (i.e., are model parameters constant over a tidal cycle?).

WORK DONE PREVIOUSLY

Mapping chlorophyll *a* concentration from interpolation among surface measurements is a difficult task, subjective at best, and some sampling stations are too shallow to permit easy access for sampling (Khorram, 1981a). As an alternative to interpolation among surface measurements, Khorram (1981a) first used Ocean Color Scanner (OCS) data composed of reflectance measurements in visible and near infra-red wavelengths acquired from a NASA U-2 overflight with simultaneous surface measurements to delineate the chlorophyll maximum in northern San Francisco Bay. Khorram later (1981b) used Landsat-3 Multispectral Scanner (MSS) digital data, along with concurrent surface measurements, to map other indices of water quality over the entire San Francisco Bay. Both studies successfully delineated the turbidity/chlorophyll maximum and Landsat-assisted mapping provided a potential

for repetitive monitoring coverage of the entire San Francisco Bay. However, some concern has arisen (among government officials) over the relatively low resolution capability (80 x 80 m) of the Landsat MSS system. In response to this concern, this research has employed a higher resolution Daedalus 1260 Multispectral Scanner (40 x 40 m), capable of recording better than twice as many wavelength channels (10 channels) over the same spectral range as the Landsat-3 MSS (4 channels). Narrowing the receiving wavelength ranges facilitates remote sensing of specific absorption and reflectance spectra characteristic of chlorophyll a.

Researchers have used a variety of remote platforms to investigate the relationship between reflected energy measured by a multispectral scanner and chlorophyll a concentration (Clarke et al., 1970; Arvesen et al., 1973; Duntley et al., 1974; Anderson and Horne, 1975; Clark et al., 1980b; Smith and Baker, 1982; Platt et al., 1983). In addition to reflected energy, the natural fluorescence of chlorophyll a at 685 nm has also been used as a basis for developing both passive and active remote monitoring systems (Bristow et al., 1979; Neville and Gower, 1977; Gower and Borstad, 1981; Hoge and Swift, 1981). Interest in global productivity/ecology has instigated several large multidisciplinary studies (i.e., Superflux, 1980; Marex, 1982) that have rapidly advanced the refinement of

sensors, statistical analysis techniques and spectral characteristics of phytoplankton color/taxonomic groups used to monitor surface chlorophyll a (Cambell and Thomas, 1981; Walsh, 1982).

The Coastal Zone Color Scanner (CZCS) is the primary sensor employed in open ocean chlorophyll a studies. It provides coverage over a large oceanic region wherein phytoplankton fields commonly range from 0-10 µg/l. Low open ocean chlorophyll a levels limit the CZCS's detection of chlorophyll a absorbance and reflectance to the blue (440 nm) and green (520 and 550 nm) portion of the electromagnetic spectrum. Atmospheric correction algorithms are also employed to reduce interference with chlorophyll a predictions (Gordon, 1980).

Coastal chlorophyll a concentrations, however, may range as high as 1000 µg/l during bloom conditions (Munday and Zubkoff, 1981). Therefore, previous remote sensing investigations of chlorophyll a in coastal environments have utilized chlorophyll a absorbance and reflectance information in the red (670 nm) and near infra-red (750 nm) as well as blue and green portions of the electromagnetic spectrum (Johnson, 1978; Kim et al., 1980; Uno et al., 1980; Grew, 1981; Johnson et al., 1981; Munday and Zubkoff, 1981; Bowker et al., 1983).

Johnson (1978) analyzed data from two multispectral scanners flown at different altitudes over two estuarine

regions with chlorophyll a ranging from 1.6 - 19.5 µg/l (n=21) in one case and from 2.2 - 24.3 µg/l (n=18) in the other. He concluded that (using a M^2S multispectral scanner) reflectance measurements from the 440 - 490 nm, 620 - 660 nm, and 700 - 740 nm wavelength regions could be used as independent variables in linear regression to estimate near surface chlorophyll a concentrations. Using OCS data, Johnson (1978) found that the 499 - 519 nm and 610 - 630 nm wavelength regions produced the closest agreement between observed and predicted values of chlorophyll a concentrations. In both cases he warned that the concentration of suspended sediments may influence the results. Later research in the New York Bight Apex employed the M^2S camera system and found a strong correlation (R=.936) between chlorophyll a values measured by a continuous shipboard fluorometer and measurements of visible and near infra-red reflectances from band 2 (440 - 490 nm) and band 4 (540 - 580 nm) (Johnson et al, 1981). Band 5 (580 - 620 nm) provided the highest correlation (R=.965) with measured concentrations of suspended matter. The 25 surface measurements were truly simultaneous since multiple overpasses of the ship were flown during its cruise. Surface measurements of chlorophyll a concentration ranged from 26 - 100 mg/m^3 while suspended sediment concentration ranged from 24 - 34 mg/l.

Kim et al. (1980) utilized a chlorophyll index composed of the ratio of the difference of 472 nm and 548 nm over the sum of these two wavelength regions as input to a non-linear model for estimating chlorophyll *a* concentrations. Ocean Color Scanner reflectance data in the visible and near infra-red portions of the electromagnetic spectrum were taken from a U-2 aircraft for an *in situ* chlorophyll *a* range of 3 - 20 µg/l (n=12). The correlation between measured chlorophyll concentration and the calculated chlorophyll index was -0.965.

Uno et al. (1980), examining reflectance data from a Daedalus 1250 MSS flown over Yashima Bay, regressed chlorophyll *a* measurements versus reflectance measured in Daedalus channel $3/\Sigma x$, where Σx = the sum of count values in Daedalus channels 2 through 9. The channel midpoints and bandwidths of the Daedalus 1250 and Daedalus 1260 MSS are identical (see Table 1). The predictor variable $3/\Sigma x$ was applicable to two different dates (n=12, 1977; n=19, 1978), flight altitudes, and tidal conditions with measured chlorophyll *a* concentration ranging from 13.2 - 71.6 µg/l. Another normalized ratio examined in this study was $7/\Sigma x$. This variable produced satisfactory statistical fits to the two data sets but was suspected to be influenced by suspended sediments.

Munday and Zubkoff (1981) observed dinoflagellate blooms in the York River, Virginia, by means of infra-red

TABLE 1. Daedalus Multispectral Scanner: channel wavelength sensitivities.

Ch. 1	380-420	nm	(ultraviolet band)
Ch. 2	420-450	nm	(violet band)
Ch. 3	450-500	nm	(blue band)
Ch. 4	500-550	nm	(green band)
Ch. 5	550-600	nm	(yellow band)
Ch. 6	600-650	nm	(orange band)
Ch. 7	650-690	nm	(red band)
Ch. 8	700-790	nm	(infrared band)
Ch. 9	800-890	nm	(infrared band)
Ch. 10	920-1100	nm	(infrared band)

and natural color aerial photography. Water samples were collected at six stations and measured chlorophyll a values ranged from 19 - 1038 µg/l. The analysis simulated the change in reflectance due to various concentration combinations of chlorophyll a and suspended sediment. The wavelength regions examined were 680 nm and 700 nm. Conclusions drawn indicated that separation and quantification of chlorophyll a and suspended sediment concentrations from color and color IR aerial photography was not possible. The researchers reiterated that below concentrations of 30 - 50 µg/l chlorophyll a reflectance in near IR wavelengths ceases to be a useful predictor (Bressette and Lear, 1973).

The Multichannel Ocean Color Sensor (MOCS) and the Test Bed Airborne Multispectral Scanner (TBAMS) are both multispectral scanners developed by NASA for the purpose of monitoring visible and near infra-red wavelengths. Real time MOCS channel 7 reflectance data (490 nm) from two consecutive days of sampling 37 sites agreed well with measured low concentrations (0 - 10 µg/l) of chlorophyll a in Chesapeake By (Grew, 1981). Bowker et al. (1983) used the TBAMS over Chesapeake Bay. Chlorophyll a concentrations at nine sites were measured with water sampling times differing from the overflight by as much as two hours. Three band ratios were regressed against measured surface concentrations of chlorophyll a.

Reflectance data from bands 3-6 (512 - 640 nm) resulted in the highest correlations in reference to surface measured chlorophyll a. Information in bands 6-8 (640 - 712 nm) provided the best fit for predicting suspended sediments. Researchers concluded that the three band ratio is insensitive to atmospheric and sun angle variations.

These studies are pertinent to this research not only in their selection of wavelengths used as model input with regard to broad chlorophyll a ranges encountered in situ, but also because suspended sediment is recognized as an influence on near surface water reflectances in the red region of the electromagnetic spectrum.

No data on the concentration of suspended sediments in each surface water sample is available for this study. It is highly probable, therefore, that suspended sediments may be influencing scanner radiance measurements in Daedalus 1260 channels 7 and 8. According to Morel and Prieur (1977) suspended sediment reflectance in wavelength regions of channels 7 and 8 are quantitatively similar. By the use of a ratio of the reflectance measured in channel 7 over that measured in channel 8 it is hoped that the radiance contribution from suspended sediments and atmospheric haze will be minimized.

An estuarine remote sensing system must not only be able to resolve chlorophyll a patchiness over a large concentration range rapidly altered by inflow and tidal

currents but also radiance contributions from atmospheric scattering (Rayleigh's Law and aerosol effects), bottom reflectance, surface reflectance, and suspended particulates (organic and inorganic).

Unfortunately, measurements of upwelling and downwelling irradiance at the water surface sample locations do not exist for this study, making quantitative partitioning of radiance influences due to the above components impossible. Therefore, this study has attempted to roughly minimize extraneous radiance influences by careful selection of band transformations used to predict chlorophyll _a_ concentrations.

A further note of interest is that in this survey of nine cases, only one sample size exceeded 25 sites. This sparse number of surface samples is characteristic of remote sensing water quality investigations due to logistics and expense.

CONSIDERATIONS IN THE SELECTION OF WAVELENGTH REGIONS USED FOR MODELING

The physical basis for the models developed in this study was derived from inspecting the literature on laboratory investigations of the spectral characteristics of phytoplankton, as well as previously successful remote sensing investigations of estuarine chlorophyll _a_.

Two marine diatom species far outnumbered (in organism/ml counts) any other phytoplankter on the day

of the overflight. All water samples taken for organism/ml counts were obtained between 11 a.m. and 1 p.m. on the day of the overflight. The two diatom species were Thalassirosora excentricus and Skeletonema costatum. During annual periods of low fresh water inflow associated with high summer phytoplankton standing crops in the Suisun Bay region, these two species frequently outnumber all others (Ball and Arthur, 1979; Arthur and Ball, 1978). A shift in size of diatomaceous chains to > 22 nm with increasing population density keeps these species in the entrapment zone by allowing them to settle downward into the landward flowing bottom current before they can be transported away from Suisun Bay in the surface layer (Cloern, 1979; Arthur and Ball, 1978).

Previous laboratory research has shown that the spectral characteristics of phytoplankton cultures depend on age, vitality, and concentration as well as taxonomic distinction (Richards et al., 1952a, b; Yentsch, 1960; Duntley et al., 1974; Wilson and Kiefer, 1979; Uno et al., 1980). All algae absorb energy in the 430 nm and 670 - 680 nm regions of the electromagnetic spectrum due to the presence of chlorophyll a (Anderson and Horne, 1975). Reported laboratory spectral curves of marine diatoms, including Skeletonema costatum, demonstrate that as chlorophyll a concentration increases, wavelengths < 500 nm and ~ 670 nm are increasingly absorbed while

wavelengths in the 550 - 600 nm range and near infrared spectral region (> 750 nm) are increasingly reflected (Anderson et al., 1975; Uno et al., 1980). See Figure 2.

Recent work at NASA, Langley (Farmer et al., 1983) involved investigations into the use of visible absorbance spectra as a basis for remote sensing of algal concentration and community composition. They found that absorbance spectra of different cultures of the same species were most similar. The separation and quantification of mixed phytoplankton color groups was possible using information from the difference between radiance measured at 680 nm and 720 nm (Daedalus channels 7 and 8).

The selection of Daedalus channel 7/8 reflectance ratio as an independent variable in the chlorophyll *a* model is based on the aforementioned spectral properties of chlorophyll *a*. The reflectances measured in Daedalus channels 7 and 8 are combined as a ratio rather than a difference in the hope that haze influence in channel 7 will tend to cancel out similar haze influence in channel 8. As chlorophyll *a* concentration increases in surface waters, less reflected energy is received in Daedalus channel 7 (650 - 690 nm) due to chlorophyll *a* absorption. On the other hand, with increasing chlorophyll *a* concentration, the reflectance in Daedalus channel 8 (700 - 790 nm) increases. It is the change in the slope of the reflectance curve from Daedalus channel 7 to

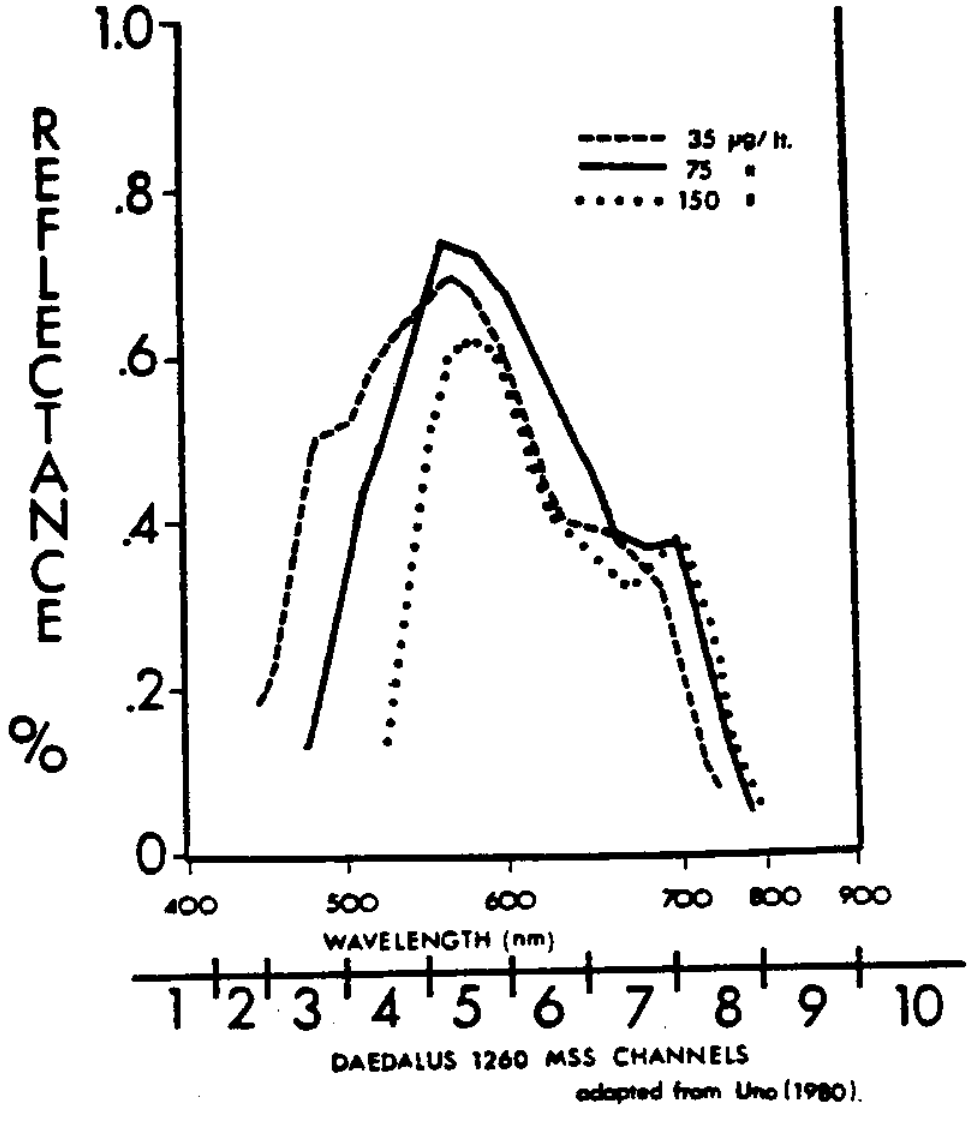

FIGURE 2. Relationship between percent reflectance and wavelength at various concentrations of Skeletonema costatum in culture.

Daedalus channel 8 with increasing chlorophyll a concentration that permits the ratio of 7/8 to be a useful predictor variable. This 7/8 ratio is most useful at higher chlorophyll a concentrations due to the increasing absorption of near infrared radiation by water reducing the intensity of the reflectance by chlorophyll a in Daedalus channel 8 when chlorophyll a is low (Morel et al., 1977; Gordon and Clark, 1980; Uno et al., 1980). To observe the increase in the value of the channel 7 over 8 reflectance ratio as chlorophyll a concentration decreases see the third and eighth columns of Tables 2 and 3.

The absorption in the blue and green wavelength regions of the spectrum (450 - 550 nm) by chlorophyll a is selected as an input variable in the model because this absorption is sensitive to changes in chlorophyll a at lower concentrations (Uno et al., 1980). The form of this variable, Daedalus channel 3 minus Daedalus channel 10, is an attempt to remove unwanted reflectance contributions from the atmospheric haze that plagued the afternoon scene. The rationale of this transformation is that most of the energy recorded by Daedalus channel 10 is atmospheric or surface reflectance since essentially near zero reflectance from the water column would occur in this wavelength region of 1000 - 1100 nm (Morel et al., 1977; Gordon et al., 1980). At the same time, absorption by chlorophyll a is taking place in Daedalus channels 2, 3,

TABLE 2. Morning ebb tide raw data. Chlorophyll *a* concentrations (ug/l), Daedalus 1260 scanner band count values and band transformations.*

Site	Time From Overflight in Min.	Observed Chlor. a	Daedalus Channel 3	Daedalus Channel 7	Daedalus Channel 8	Daedalus Channel 10	Ratio Daedalus Channel 7 to Channel 8	Daedalus Channel 3 Minus Channel 10
1	0	14.4	43.96	48.28	42.28	27.36	1.14191	16.60
2	0	9.3	44.00	48.92	42.36	27.40	1.15486	16.60
3	5	9.0	44.04	48.20	41.00	27.44	1.17561	16.60
4	45	33.0	44.04	47.56	41.08	25.52	1.15774	18.52
5	25	20.0	44.20	50.40	44.24	27.60	1.13924	16.60
6	35	28.2	44.36	52.44	48.80	30.92	1.07459	13.44
8	40	66.0	44.92	51.64	48.36	29.96	1.06782	14.96
9	50	23.9	44.76	49.64	43.04	26.40	1.15335	18.28
10	63	22.9	44.04	49.60	42.72	25.72	1.16105	18.32
11	-13	60.5	47.04	53.00	51.00	28.96	1.03759	18.08
12	0	49.5	46.00	51.92	48.80	27.84	1.06219	18.16
13	0	24.4	44.96	47.00	39.76	23.00	1.18410	21.96
14	-10	55.7	47.16	51.36	48.96	28.32	1.04902	18.84
15	0	66.0	47.52	52.96	51.04	28.40	1.03762	19.12
17	20	24.0	45.92	50.92	46.60	25.32	1.09083	20.60
18	13	35.0	45.04	51.20	47.44	25.90	1.07926	19.14
19	55	37.0	44.60	51.36	46.16	29.04	1.11265	15.64
20	65	16.4	44.72	51.12	45.00	28.36	1.11616	16.36
21	60	49.5	44.04	50.20	45.92	27.95	1.09495	16.09
22	71	39.9	44.32	52.76	49.52	31.20	1.06543	13.04
23	55	38.5	44.20	52.00	47.32	29.44	1.09890	14.76
24	-13	34.4	44.96	53.00	51.20	31.70	1.05070	13.26
25	0	53.6	44.96	52.40	49.24	30.64	1.06413	14.32
26	50	33.7	44.92	52.24	48.00	32.20	1.08652	12.64
27	50	27.5	45.04	51.76	46.00	31.40	1.12522	13.56
28	-37	27.3	44.76	51.00	46.36	32.12	1.10101	12.64
29	0	26.1	44.04	53.00	49.00	32.04	1.06255	11.20
30	0	17.2	43.16	50.76	45.60	30.36	1.11316	12.80
31	15	14.6	44.04	51.56	44.92	27.00	1.14782	16.16
32	24	11.5	44.12	51.04	44.40	28.00	1.14955	16.12
33	-42	31.6	44.60	51.00	48.12	29.20	1.07814	15.48
34	-20	39.9	44.00	52.00	50.64	30.72	1.02686	13.28
35	20	32.2	44.00	50.00	46.76	27.00	1.06929	16.12
36	31	48.1	44.00	49.52	46.40	27.60	1.06540	16.40
37	24	20.2	45.00	53.00	51.44	32.60	1.04743	12.40
38	30	36.4	45.00	52.04	47.52	29.00	1.11195	16.00
39	-16	22.1	44.00	52.04	48.32	31.70	1.07699	12.30

* Count values were derived by quantizing spectral radiance (Lλ) to 8 bit digital counts.

TABLE 3. Afternoon flood tide raw data. Chlorophyll *a* concentrations (ug/l), Daedalus 1268 scanner band count values, and band transformations.*

Site	Time From Overflight in Min.	Observed Chlor. a	Daedalus Channel 3	Daedalus Channel 7	Daedalus Channel 8	Daedalus Channel 10	Ratio Daedalus Channel 7 to Channel 8	Daedalus Channel 3 Minus Channel 10
1	0	10.0	61.00	75.56	74.00	69.36	1.00900	-7.40
2	5	12.1	60.60	71.64	70.00	66.12	1.02226	-5.52
3	15	12.0	60.72	74.52	74.96	69.76	0.99413	-9.04
4	59	12.6	64.00	77.00	79.32	71.12	0.98185	-6.24
5	30	22.7	59.00	71.12	69.72	61.40	1.02000	-2.40
6	40	22.4	58.32	70.76	69.72	61.20	1.01492	-2.00
7	29	44.0	58.16	70.00	69.76	54.52	1.00344	3.64
8	43	21.3	61.92	75.00	76.16	65.32	0.99527	-3.40
9	69	16.2	60.20	72.64	71.20	61.72	1.01900	-1.52
10	00	19.0	60.12	73.36	72.16	62.40	1.01663	-2.28
11	-21	64.6	62.36	76.32	79.84	61.40	0.95591	0.00
12	-5	46.0	61.52	74.64	75.04	59.40	0.98410	2.12
13	55	41.3	59.96	71.96	71.40	55.72	1.00672	4.24
14	-11	65.3	62.92	76.24	79.64	60.20	0.95731	2.64
15	0	75.7	62.32	75.96	78.40	59.40	0.96709	2.04
16	3	50.5	60.00	73.64	75.20	56.60	0.97926	4.20
17	10	64.0	60.72	73.16	74.04	55.16	0.97755	5.56
18	15	66.0	57.00	69.00	70.40	51.92	0.99149	5.96
19	60	31.0	52.04	63.24	62.24	48.96	1.01607	3.00
20	95	25.4	51.44	62.40	61.00	47.04	1.02295	4.40
21	65	46.1	51.76	62.00	61.40	47.64	1.00046	4.12
22	64	42.6	51.12	62.00	60.60	45.60	1.03626	5.44
23	50	37.1	51.92	63.92	61.44	45.32	1.04036	6.60
24	-40	33.0	51.60	63.60	62.64	46.20	1.01660	5.40
25	-20	31.6	51.00	62.92	61.40	45.92	1.02342	5.00
26	01	34.4	51.00	64.44	64.00	48.00	1.00607	3.00
27	-06	14.6	51.00	64.04	62.20	47.16	1.02950	3.84
28	-60	11.6	50.20	62.92	61.76	47.60	1.01070	2.60
29	-30	6.0	52.00	65.44	64.52	50.24	1.01426	1.76
30	-20	11.6	51.12	64.24	60.00	46.36	1.05519	4.76
31	-0	9.2	50.00	63.20	60.72	43.36	1.04004	6.72
32	0	0.7	49.00	62.04	56.96	40.44	1.00919	9.44
33	-65	37.1	51.04	61.56	59.96	44.50	1.02660	6.40
34	-55	31.6	50.60	60.04	59.44	44.64	1.01009	5.96
35	22	49.5	52.72	62.00	62.00	49.10	1.00000	3.62
36	30	55.7	51.44	61.00	65.00	51.04	0.94043	-0.40
37	-7	44.0	51.04	64.44	63.72	45.76	1.01130	5.20
38	0	30.5	52.40	65.16	65.44	40.00	0.99572	4.32
39	-55	10.0	52.00	66.20	67.20	54.00	0.98514	-2.00

* Count values were derived by quantizing spectral radiance (LA) to 8 bit digital counts.

and 4 (Anderson et al., 1975; Uno et al., 1980). As chlorophyll *a* concentration increases, the slope between reflectance values in Daedalus channels 2 and 4 moves in a positive direction (Uno et al., 1980). Reflectance from channel 2 minus that from 10, channel 3 minus 10, and channel 4 minus 10 were all examined as possible variable transformations during the regression modeling. Reflectances measured for Daedalus channel 2 to 4 were also used alone and combined as ratios during independent variable selection. The transformation 3 minus 10 applied most consistently to both morning and afternoon data sets. For this reason, it is concluded that for these particular data the proportion of atmospheric interference in Daedalus channel 3 reflectance was most completely removed by subtracting the value of Daedalus channel 10 reflectance. In any case, development of future models capable of consistent predictions of surface chlorophyll *a* concentrations must be based on simultaneous measurements made of surface irradiance (upwelling and downwelling) and scanner spectral value comparisons.

RESEARCH METHODOLOGY

The research approach involved (1) simultaneous acquisition of near surface measurements of water quality from boats and airborne Daedalus 1260 Multispectral Scanner (MSS) visible and near infra-red reflectance

measurements; (2) chlorophyll *a* laboratory analysis of whole water samples from 39 sites; (3) extraction of digital count values from Daedalus scanner for 39 sample sites; (4) bad data replacement; (5) development of regression equations relating Daedalus MSS data to chlorophyll *a* measurements; and (6) transformation of Daedalus 1260 MSS data through selected best-fit regression models for production of surface chlorophyll *a* distributions for the entire study area.

Collection of Near Surface Water Samples and Laboratory Analysis for Surface Chlorophyll *a* Concentrations

On August 28, 1980, chlorophyll *a* concentration was sampled by collecting water samples in bottles at 39 sites from 5 boats. The 39 sample sites were chosen arbitrarily to give the greatest possible areal coverage of the study area considering the limited numbers of boats and personnel measuring surface conditions. Sampling was conducted throughout the day with each boat responsible for a number of sample sites along a designated transect. All samples were taken at a depth of 3 feet below the surface. The vertical distribution of phytoplankton in the top meter of water in the study area is characteristically homogeneous (Dr. Cloern, personal communication). Location of the sample sites is shown in Figure 1. Sampling times were recorded and water samples collected at times closest to the Daedalus scanner

overflight were used in the equation development. All water samples were acquired within 1.5 hours of the scanner overflight.

Water samples were collected onto glass fiber filters which were extracted in 95% acetone. Chlorophyll *a* concentration was determined fluorometrically (Strickland and Parsons, 1972) from acetone extracts. These values were corrected for phaeopigments. Chlorophyll *a* concentrations and extracted count values for the 39 sample sites for the morning overflight are displayed in Table 2, and for the afternoon overflight in Table 3. Count values represent a rescaling of the original voltages produced by the multispectral scanner to a scale ranging from 0 to 127.

Acquisition and Processing of Daedalus MSS Data

From 8:30 - 8:45 a.m. and from 3:00 - 3:15 p.m. (PDT) of August 28, 1980, two NASA U-2 overflights of the study area were flown at approximately 55,000 ft. in conjunction with ebb and flood tide conditions, respectively. Overflight times corresponded closely with the highest and lowest water conditions of the study area that day (see Figure 3). An altitude of 55,000 ft. produced a ground resolution cell of 42 x 42 m using the Daedalus 1260 Multispectral Scanner (angular resolving power of 2.5 mrad). The Multispectral Scanner recorded 10 channels of

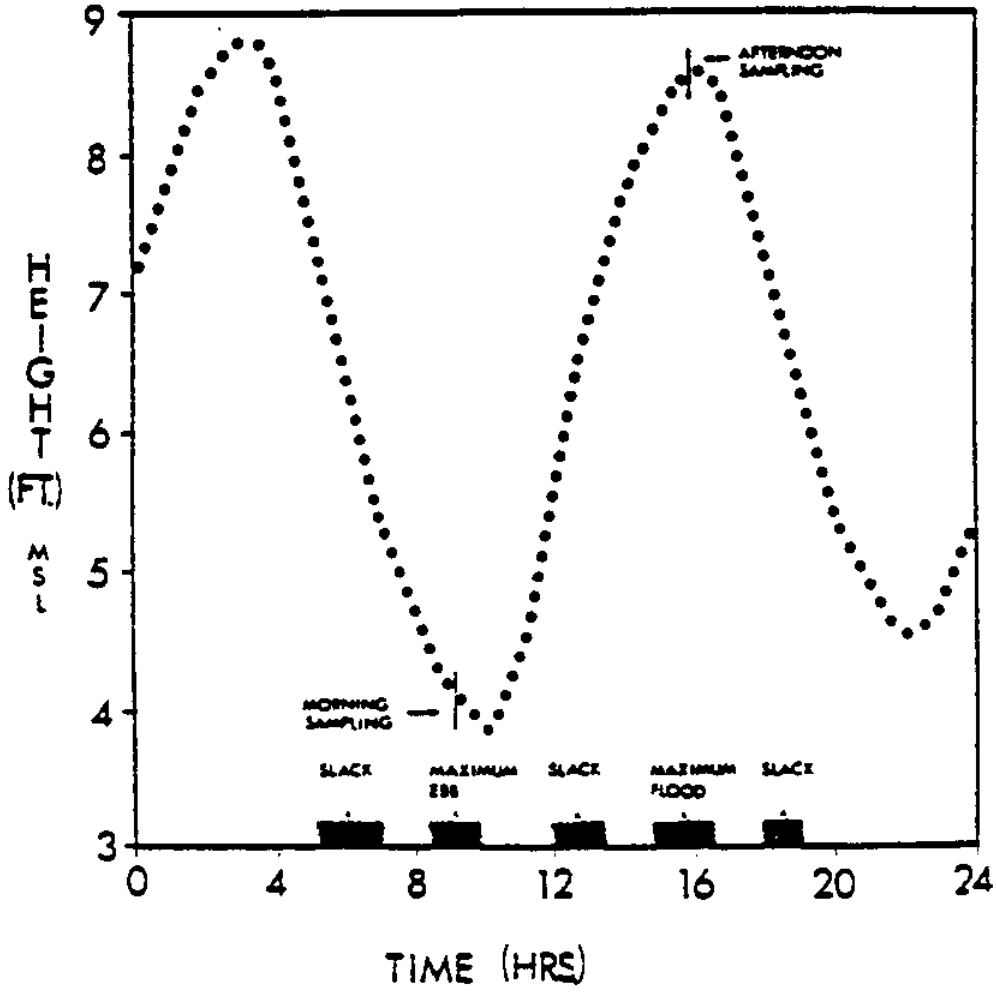

FIGURE 3. The rise and fall of the tide on the day of sampling within the study area. Vertical lines indicate the approximate time of simultaneous overflight and near surface water sampling. The dotted line represents water height above mean sea level (MSL).

reflected energy and two channels of thermal imagery. Only the reflected wavelengths were considered in this study (see Table 1).

In order to extract the count values of each scene for the corresponding 39 water sample sites, a second order polynomial regression equation was developed. This equation regressed control points from USGS topographic maps using a Universal Transverse Mercator (UTM) grid system against the same control point located visually on the imagery. Regression residuals were examined and sample sites were verified visually. In this fashion, the scanner imagery was mathematically transformed to conform to the latitudinal and longitudinal coordinates of ground sample site locations.

To ensure the proper location of sample sites, a block of 5 pixels by 5 pixels surrounding each sample site was located and the average count values computed. These mean count values were then used in developing chlorophyll *a* concentration prediction models. The squares outlined in Figure 4 represent the 5 x 5 pixel blocks (approx. 200 m x 200 m) for sample sites 4, 5, 6, 8, 9, 10, 11, 12, 13, and 14 in Suisun Bay. This averaging procedure was done for both the morning and afternoon scenes. Standard deviations of count values for all wavelength channels in each pixel block ranged from $\pm$ 0 - 4%.

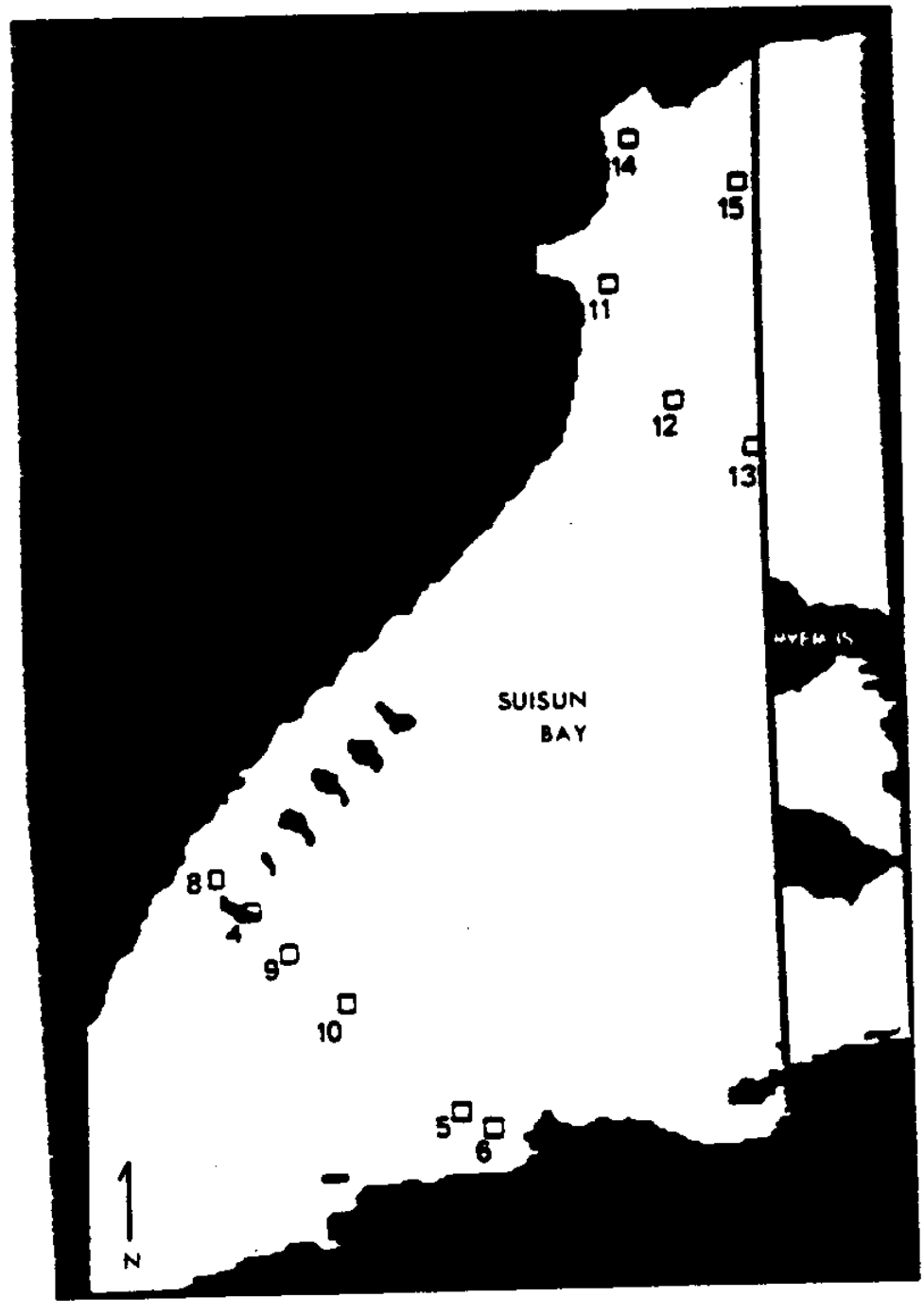

FIGURE 4. Relative size of 5 x 5 pixel blocks representing 200 m x 200 m on the ground. Discontinuity truncating the western end of the islands at right is scan dropout region of approximately 30 missing lines. Note image scalloping affecting northern shoreline of Suisun Bay and the Mothball Fleet.

Bad Data Replacement

It was not possible to use the previously described method of count value extraction for the morning ebb tide scene. During the morning overflight, severe turbulence was encountered causing tilting of the aircraft. This pitch manifests itself on the imagery by slightly altering the ground distance from one scan line to another. This is visible in Figure 4 as a scalloped shoreline. (Also, note the sickle shapes of the normally rectangular moth ball fleet.) The turbulence was unsystematic and randomly variable throughout the scene. Attempting to mathematically transform this image to overlay it with the afternoon scene or register it to a UTM projection was impossible with the available software. Instead, the sample points were located by triangulation and visual verification techniques. Scan start problems dropped 30 lines of data over Suisun Bay during the morning overflight. Radiance values for two sample sites from the morning scene were lost to this malfunction (sites 7 and 16). Final output products have a black filler region spacing the scene correctly and indicating the area of data loss.

The afternoon scanner overpass had scan line starting problems in Daedalus channel 10. These appear on analog imagery as lines of offset densities (i.e., land values offset over water and vice versa). An algorithm

interpolating across these bad scan values by assigning the average of the preceding and subsequent scan lines to the bad line was used for correction. There were 80 bad scan lines in the morning scene out of 1080 total lines (7.5%).

Model Development

The modeling approach involved two sets (morning and afternoon) of near surface chlorophyll a concentration measurements and two sets of scanner data. The chlorophyll a were used as dependent variables while the independent variables were composed of simple functions of reflectance measurements recorded as count values of selected channels of the Daedalus scanner. The "best fit" single model for predicting chlorophyll a concentration in both morning and afternoon scenes was chosen on the basis of significance and stability of the overall model and of its coefficients. Criteria examined in order to compare various models included R^2 values, F-test results of the significance of the overall model, t-test results of the significance of the coefficient estimates, standard errors of the overall model and each of its coefficients, and residual analysis.

Prior to the use of spectral data in modeling, histograms of the count values for both scenes were examined (see Figure 5). The histogram of morning scene count values appears as a normal distribution while the

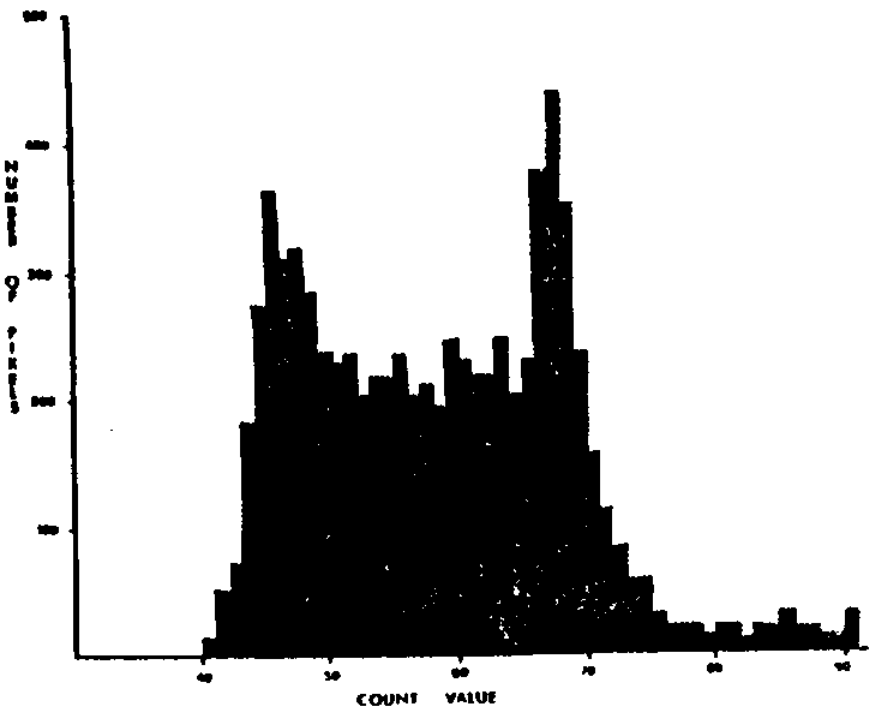

FIGURE 5a. Distribution of count values in Channel 10 for resampled file of morning ebb tide scene.

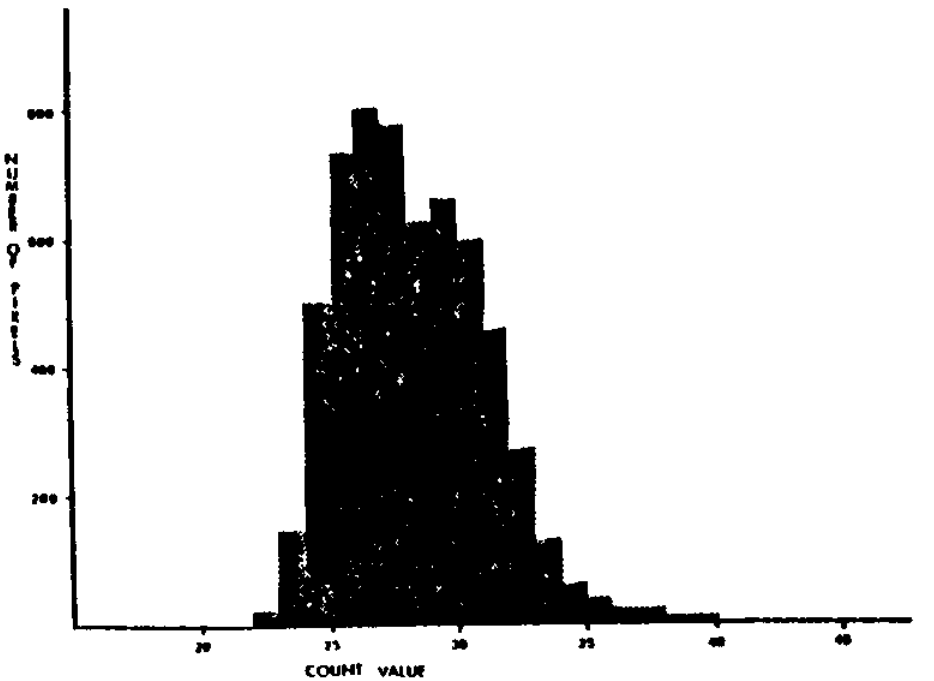

FIGURE 5b. Distribution of count values in Daedalus Channel 10 for resampled file of afternoon flood tide scene.

histogram of the afternoon scene displays a marked bimodal tendency. Upon closer inspection, the bimodal condition of the afternoon scene was attributable to the influences of a thin wedge of haze covering the western third of the imagery and barely detectable on analog imagery. The haze was thickest (but not visually obstructing) over the westernmost portion of the scene and gradually diminished in thickness until it appeared to be absent east of the three islands in the center of the scene. Backscattered radiance from the haze gave haze-influenced sites higher count values in all Daedalus MSS channels (see Figure 6 and Table 4). Daedalus MSS channel 1 (ultraviolet) was removed from analysis due to the extreme degree of atmospheric scattering.

The regression modeling strategy used 30 sample sites from the morning ebb tide data set (n=37) and 30 sample sites from the afternoon flood tide data (n=39). Chlorophyll *a* concentrations from these two groups of 30 sites were modeled independently for the purpose of discovering a functional model applicable to both data sets. Seven sites were saved from the morning data for verification of the model and nine sites were saved for verification in the afternoon case. Sites saved for verification were chosen randomly after being stratified by boat location and water depth. The summary of modeling and verification regressions appears in Table 5, and plots

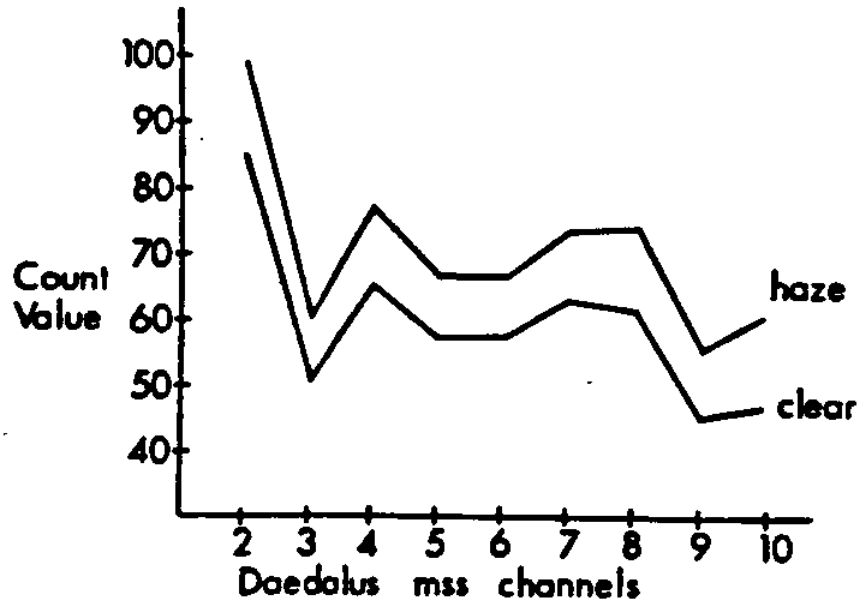

FIGURE 6. Effect of haze on mean count values of Daedalus Channels 2 through 10 during the afternoon overflight.

TABLE 4. The mean, standard deviation, and range of count values for the 18 haze-influenced and 21 clear sites.

PM HAZE SITE COUNT VALUES (N=18)				PM CLEAR SITE COUNT VALUES (N=21)			
Daedalus Channels	Mean	Standard Deviation	Range	Daedalus Channels	Mean	Standard Deviation	Range
2	99.5	2.45	95.20-94.80	2	85.0	1.65	81.85-88.25
3	60.6	1.79	57.30-64.30	3	51.2	.72	49.80-52.60
4	74.0	2.08	72.95-80.65	4	65.5	.81	64.05-66.95
5	66.3	1.62	63.35-69.25	5	57.4	.83	55.80-59.00
6	66.3	1.70	63.35-69.25	6	57.9	1.13	55.60-60.20
7	73.6	2.39	69.60-77.60	7	62.9	1.23	60.20-65.60
8	74.1	3.63	69.05-79.15	8	61.7	1.97	57.30-66.10
9	55.7	3.03	50.90-60.50	9	45.2	2.03	40.75-50.15
10	61.3	5.46	51.70-70.90	10	46.6	2.61	40.90-51.30

TABLE 5. Statistical summary of model development.

Morning ebb tide results.

	R SQUARED	F/PROB>F	RMSE	MODEL COEFS.	COEF. STD. ERROR	PROB>|T|
MODEL DEVELOPMENT (n=30)	.62	22.4/.0001	9.872	a = 123.7	46.9	.0021
				b = 2.4	0.8	.0050
				c = -299.2	45.0	.0001
Model using only sites within 15 minutes of scanner overpass (n=13)	.90	42.8/.0001	7.036	a = 365.7	41.6	.0001
				b = 3.1	0.7	.0014
				c =-349.1	38.9	.0001

Afternoon flood tide modeling results.

	R SQUARED	F/PROB>F	RMSE	MODEL COEFS.	COEF. STD. ERROR	PROB>|T|
MODEL DEVELOPMENT (n=30)	.74	39.174/.0001	9.944	a = 578.8	65.7	.0001
				b = 3.1	0.5	.0001
				c = -541.2	65.7	.0001
Model using only sites within 15 minutes of scanner overpass (n=13)	.89	48.785/.0001	9.068	a = 676.4	76.9	.0001
				b = 2.4	0.5	.0005
				c = -648.4	76.9	.0001

MODEL OF THE FORM . . . CHLOROPHYLL $\underline{a}$ (mg/l) $= a + b(x) + c(x_1)$

where x_1 = Daedalus channel 3 minus Daedalus channel 10

x_2 = Daedalus channel 7 divided by Daedalus channel 8

of predicted vs. observed chlorophyll a concentrations appear in Figure 7a and 7b. Additionally, the model was fit only to sites where near surface measurements of chlorophyll a concentration were made within 15 minutes of the scanner overflight. The necessity for surface measurements to be made as close to the overflight time as possible is demonstrated in the improved fit of these regressions (see Table 5). An attempt to include time away from overflight in minutes as an independent variable in the regression equation was made with little success. Removal of sites more than 15 minutes away from the overflight, however, did increase agreement between predicted and observed chlorophyll a concentrations as measured by the multiple correlation coefficient (R^2). The improved fit of the regression using data partitioned by nearness of time to the overflight is due partially to the reduction in number of sample sits fitted, but also because much of the influence of the time samples were taken has been removed from the regression. The influence of time on the results of regression equations is seen in the residual vs. observed plots for ebb and flood tide regression equations developed using 30 sample sites. The serial trend of these plots is apparent in Figure 8a and 8b. Plots of residual vs. observed values from regressions using data partioned by time show no trend and an improvement in overall fit (See Figure 9a and 9b, and

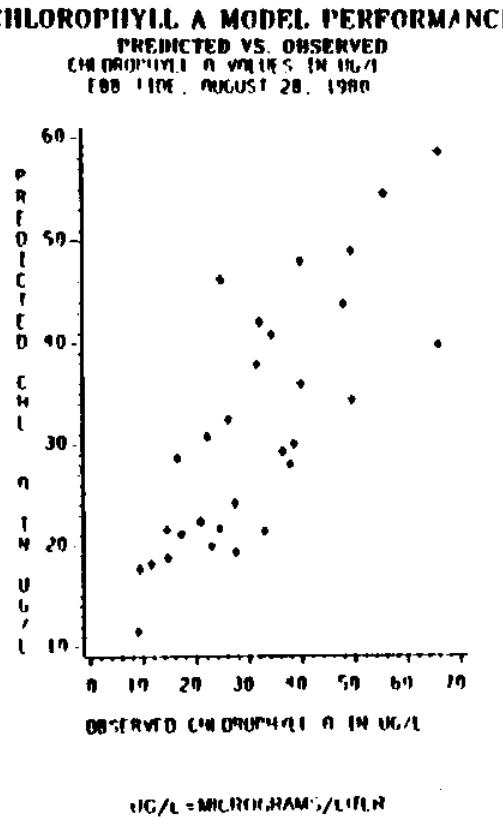

FIGURE 7a. Morning ebb tide regression using 30 sample site input.

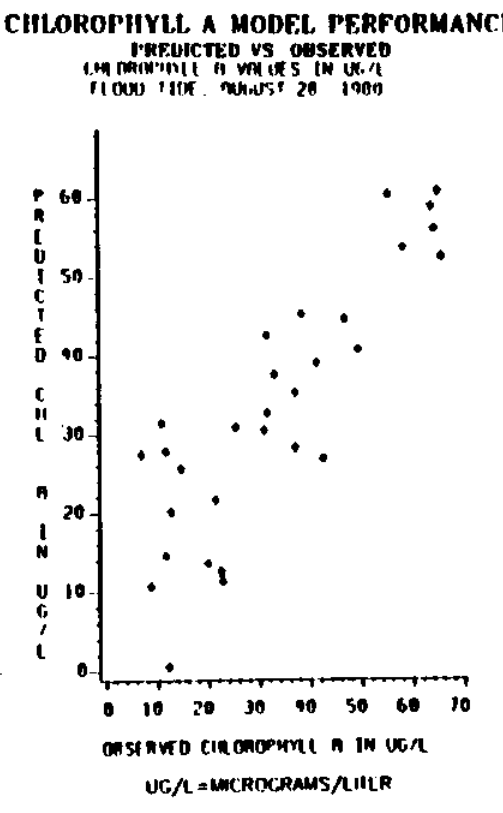

FIGURE 7b. Afternoon flood tide regression using 30 sample site input.

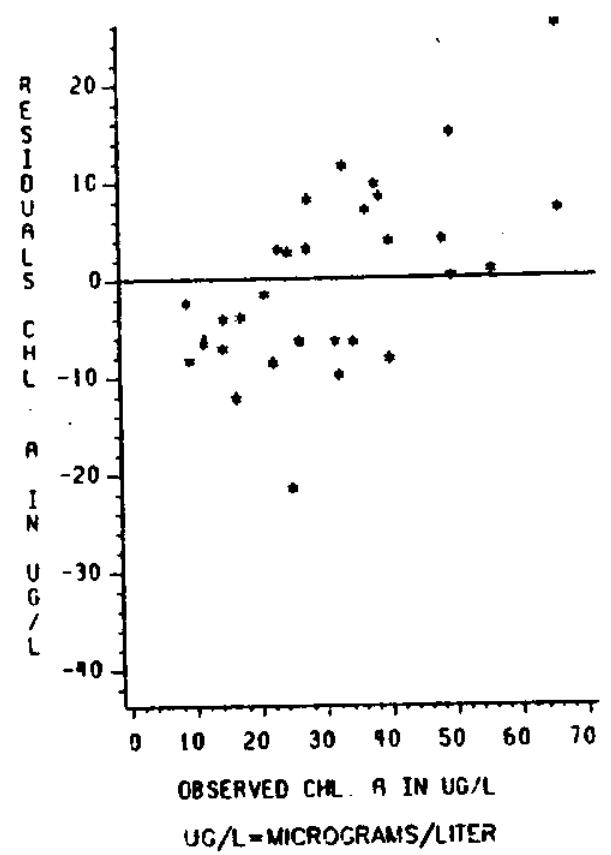

FIGURE 8a. Plot of residual vs. observed chlorophyll a concentrations for morning ebb tide regression displaying serial trend.

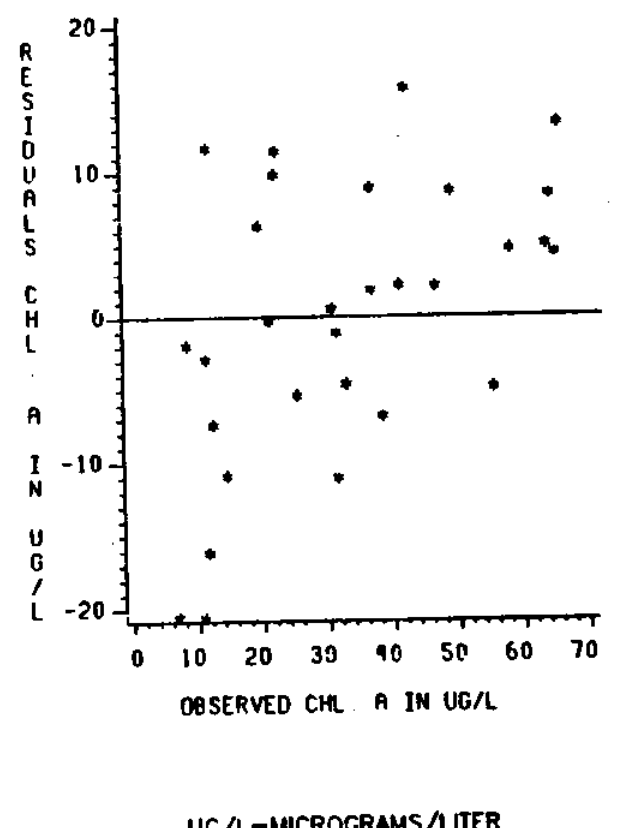

FIGURE 8b. Plot of residual vs. observed chlorophyll a concentrations for afternoon flood tide regression displaying serial trend.

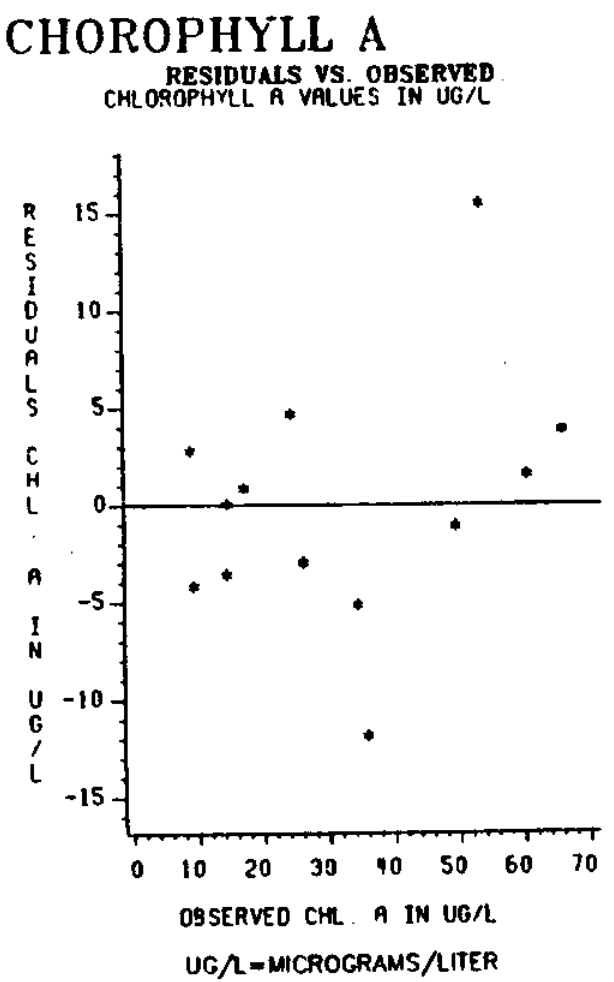

FIGURE 9a. Plot of residual vs. observed chlorophyll a concentrations for morning ebb tide regression using only sites within 15 minutes of scanner overflight. Note random dispersion about residual zero axis.

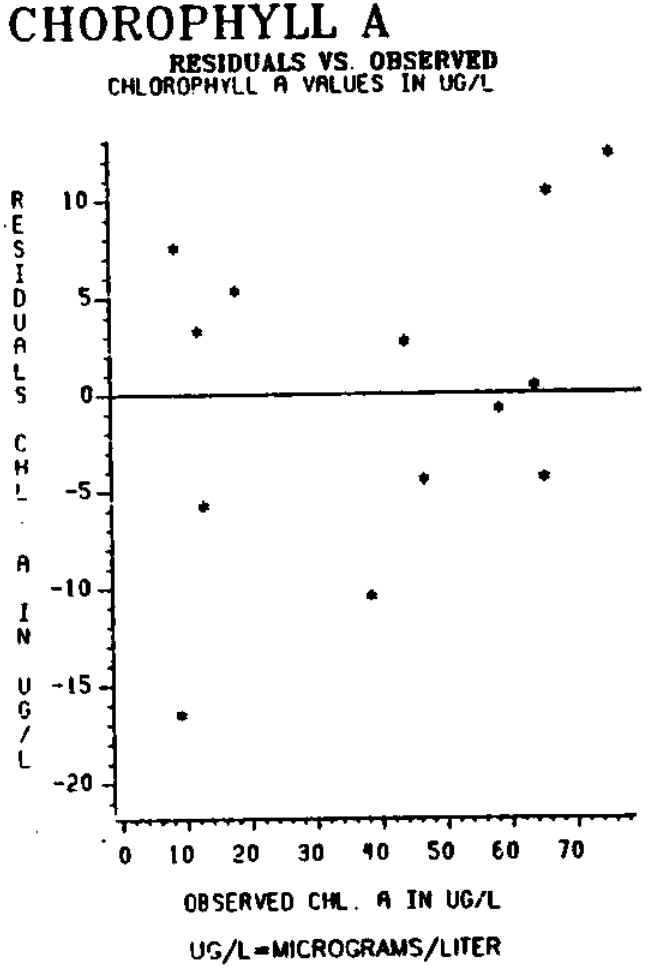

FIGURE 9b. Plot of residual vs. observed chlorophyll a concentrations for afternoon flood tide regression using only sites wtihin 15 minutes of scanner overflight. Note random dispersion about residual zero axis.

Table 5). Verification of models involved predicting chlorophyll *a* concentrations using the linear equations developed for 30 sites for ebb and flood tide data by entering the measured reflectances of the 7 ebb tide and 9 flood tide sites not used in equation development. The amount of agreement between predicted and observed values for the verification data can been seen in Tables 6 and 7. A measure of the percent variation due to chance (R^2) signifies that in all modeling and verification data from 62% - 90% of the variation in the observed chlorophyll *a* values can be explained by the models.

Plots of residual vs. predicted chlorophyll *a* concentrations appear in Figure 10 for ebb and flood tide models developed from 30 sites. The residual plots display a random dispersion about the residual zero axis and indicate that the variance of predicted chlorophyll *a* is constant throughout the predicted range. The same random dispersion is observed in plots of residual vs. predicted values for regresson equations developed using sites measured within 15 minutes of overflight.

Application of Regression Models to the Entire Study Area

All morning and afternoon models were displayed for visual inspection of spatial distributions of predicted near surface chlorophyll *a* concentrations and then compared with interpolated spatial distributions from

TABLE 6. Verification of morning ebb tide model (n=7).

Using: Chlorophyll *a* µg/l = 323.7 + 2.4 (Daedalus channel 3 minus Daedalus channel 10) - 299.2 (Daedalus channel 7 divided by Daedalus channel 8)

to predict chlorophyll *a* concentrations for 7 sites saved for verification.

SITE #	OBSERVED CHLOROPHYLL *a* (µg/l) (Y_i)	PREDICTED CHLOROPHYLL *a* (µg/l) ($\hat{Y}_i$)	RESIDUALS (e_i) ($Y_i - \hat{Y}_i$)
6	28.2	34.4	- 6.2
9	23.9	22.5	1.41
11	60.5	56.7	3.9
18	35.8	46.7	-10.9
25	53.6	39.7	13.9
26	33.7	29.0	4.8
37	28.2	40.1	-11.9
n=7	$\Sigma Y_i = 263.9$ $\bar{Y} = 263.9/7 = 37.7$	$\Sigma \hat{Y}_i = 269.0$	$\Sigma e_i = -5.18$

$$\text{Pseudo } R^2 = \frac{\sum_{i=1}^{n} (\hat{Y}_i - \bar{Y})^2}{\sum_{i=1}^{n} (Y_i - \bar{Y})^2} = \frac{\text{sum of squares due to regression}}{\text{sum of squares about the mean}} = \frac{768.5344}{1163.2000} = .66$$

The seven sites were not included in developing the regression equation used. This is not the usual method of comuting an R^2 value for a regression equation, hence the designation of pseudo R^2.

TABLE 7. Verification of afternoon flood tide model (n=9).

Using: Chlorophyll *a* µg/l = 570.8 + 3.1 (Daedalus channel 3 minus Daedalus channel 10) - 541.2 (Daedalus channel 7 divided by Daedalus channel 8)

to predict chlorophyll *a* concentrations for 9 sites saved for verification.

SITE #	OBSERVED CHLOROPHYLL *a* (µg/l) (Y_i)	PREDICTED CHLOROPHYLL *a* (µg/l) ($\hat{Y}_i$)	RESIDUALS (e_i) ($Y_i - \hat{Y}_i$)
1	18.0	1.5	16.5
3	12.8	4.8	8.1
7	44.0	39.0	5.0
9	16.2	14.6	1.6
15	75.7	55.8	20.1
21	46.1	37.8	8.3
26	34.4	35.2	- 0.78
11	9.2	28.3	-19.1
17	44.0	39.9	4.2
n=9	ΣY_i = 300.4 $\bar{Y}$ = 300.4/9 = 33.4	$\Sigma \hat{Y}_i$ = 256.8	Σe_i = 43.65

$$\text{Pseudo } R^2 = \frac{\sum_{i=1}^{n} (\hat{Y}_i - \bar{Y})^2}{\sum_{i=1}^{n} (Y_i - \bar{Y})^2} = \frac{\text{sum of squares due to regression}}{\text{sum of squares about the mean}} = \frac{2813.0240}{3719.2956} = .76$$

The nine sites were not included in developing the regression equation used. This is not the usual method of comuting an R^2 value for a regression equation, hence the designation of pseudo R^2.

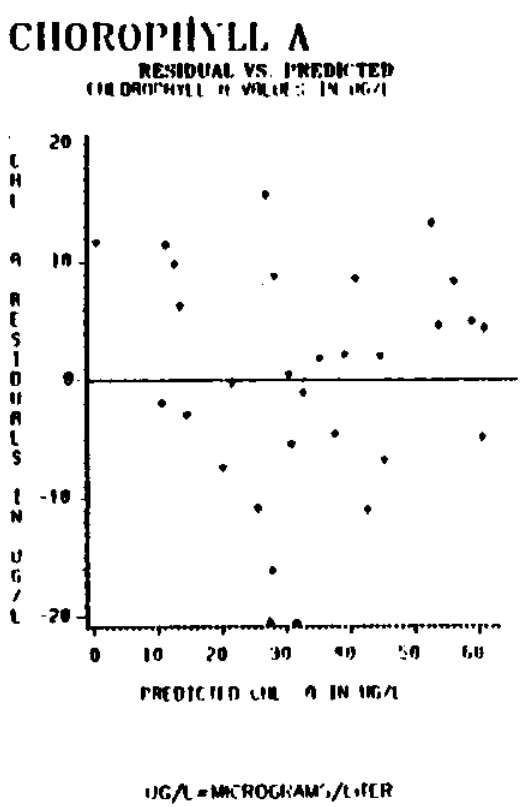

FIGURE 10a. Morning ebb tide; plot of residuals vs. predicted values of chlorophyll a.

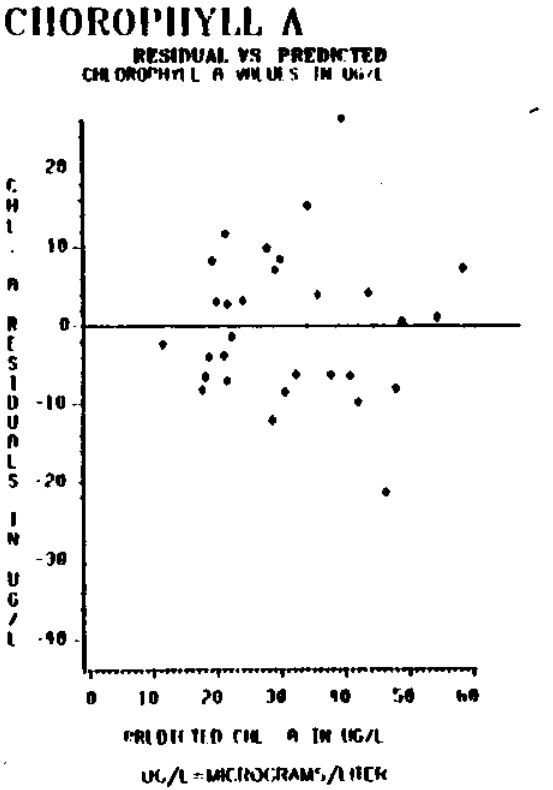

FIGURE 10b. Afternoon flood tide; plot of residuals vs. predicted values of chlorophyll a.

conventional surface surveys. Models that passed visual inspection were then extended to the entire scene including portions of the estuary not within the study area. Model applications were accomplished by using a simple linear discriminant function. By applying this function to each pixel in the study area and then grouping continuous chlorophyll a concentration predictions into discrete classes, the classification was accomplished. These discriminant functions were applied to the Daedalus MSS data to produce classified chlorophyll a surface concentration maps. These classified maps were then renumbered to produce the final maps (see Figure 11).

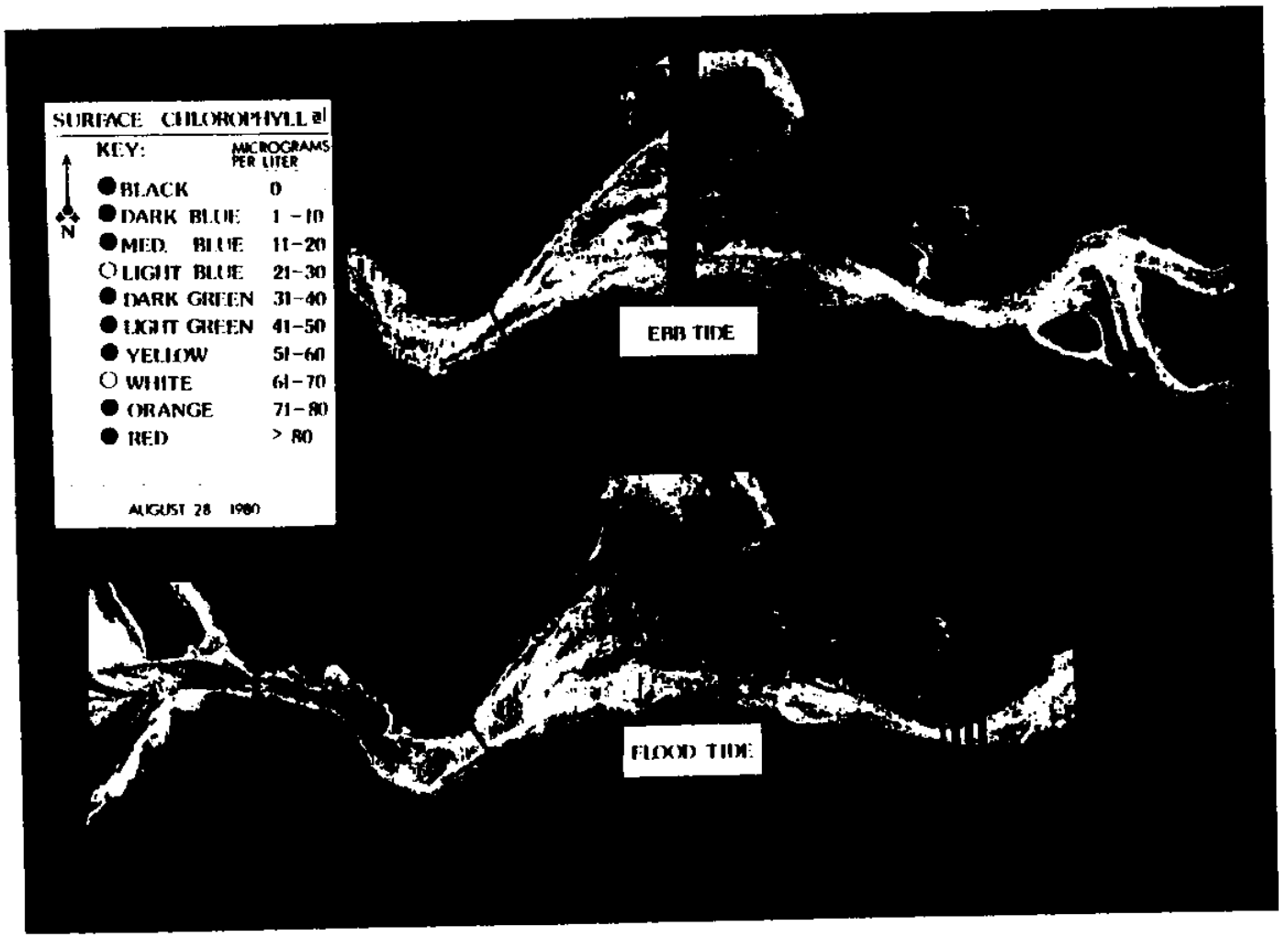

FIGURE 11. Color-coded map of surface chlorophyll a concentration during ebb and flood tide in the northern portion of San Francisco Bay, August 28, 1980.

DISCUSSION OF RESULTS

The results of this research include:

(1) a record of chlorophyll *a* concentrations at the 3 foot water depth for all 39 sample sites during the morning ebb and afternoon flood tide of August 28, 1980;

(2) a series of mathematical models developed from point sample data for the purpose of predicting surface chlorophyll *a* values at ebb and flood tide; and,

(3) color coded maps of morning and afternoon surface chlorophyll *a* concentrations of the entire study area created by applying the mathematical models developed from 30 point samples.

MORNING EBB TIDE MODEL

Chlorophyll *a* ($\mu g/l$) = $323.7 + 2.4 (x_1) - 299.2 (x_2)$

where: x_1 = Daedalus Channel 3 minus Daedalus Channel 10.

where: x_2 = Daedalus Channel 7 divided by Daedalus Channel 8.

AFTERNOON FLOOD TIDE MODEL

Chlorophyll *a* ($\mu g/l$) = $570.8 + 3.1 (x_1) - 541.2 (x_2)$

where: x_1 = Daedalus Channel 3 minus Daedalus Channel 10.

where: x_2 = Daedalus Channel 7 divided by Daedalus Channel 8.

Multispectral data from the Daedalus 1260 scanner (or Thematic Mapper) can be used to map horizontal distributions of phytoplankton biomass (chlorophyll *a*) in shallow and turbid waters such as northern San Francisco Bay. A simple regression model that uses count values from four wave bands can predict chlorophyll *a* distribution almost as accurately as field techniques based upon measurement of *in vivo* fluorescence. During this study, for example, we measured *in vivo* fluorescence (Turner Designs Model 10 fluorometer) from near surface water samples collected at sites 4, 7, 8, 9, 10, 11, 12, and 13 during five stages of the tide on August 28. Linear regression of chlorophyll *a* against *in vivo* fluorescence is a common method for predicting chlorophyll *a*, and in this instance the fit of chlorophyll *a* to *in vivo* fluorescence (see Figure 12) was not much better than that of fits to Daedalus MSS data.

Predicted horizontal distributions of chlorophyll *a* (Figure 11) for the estuarine water of the study are consistent with gross horizontal distributions inferred from boat sampling. For example, field sampling has consistently shown that chlorophyll concentration is higher in discrete water samples collected over the northern shallows of Suisun Bay than in the deeper channels (Cloern et al., 1983), and that chlorophyll concentration is usually highest in that reach of the

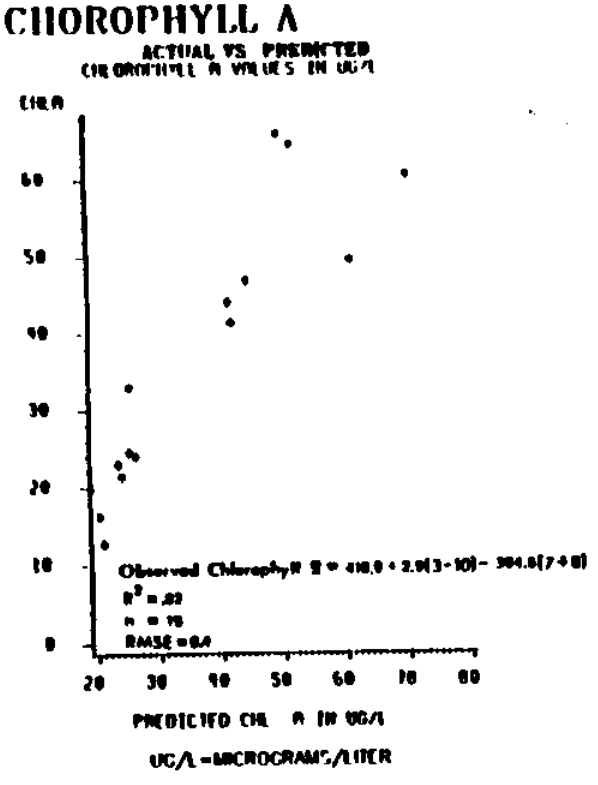

FIGURE 12a. Plot of observed chlorophyll a concentration vs. model predictions for sites 4, 7, 8, 9, 10, 11, 12, and 13 using both morning and afternoon data.

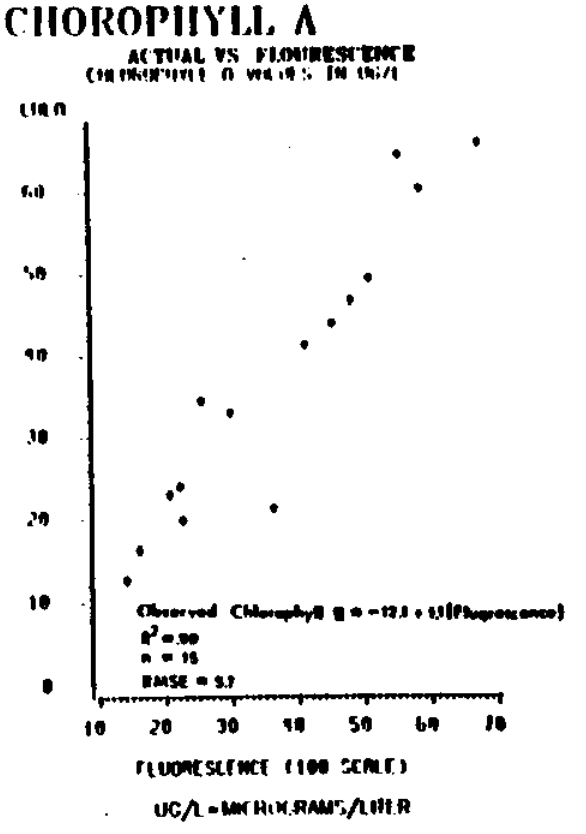

FIGURE 12b. Plot of observed chlorophyll a concentration vs. fluorescence for sites 4, 7, 8, 9, 10, 11, 12, and 13 as recorded by a continuous shipboard fluorometer for both ebb and flood tide.

channel adjacent to the northern shoals. Both of these features are apparent from Daedalus imagery, but the spatial resolution available from the application of remote sensing is much greater than has been possible from field surveys. Thus, results of this study offer the first accurate views of the two-dimensional structure of phytoplankton distribution in this estuary. Moreover, sequential flyovers provide a tool for examining the dynamic nature of the phytoplankton maximum. For example, the tidal advection of high-chlorophyll water from the northern shoals into the main body of Suisun Bay on low (flooding) tide is apparent (Figure 11) and this spatial pattern is consistent with the hypothesis that shallow waters are the source of new phytoplankton biomass (Cloern et al., 1983).

Results of this study show the potential for Thematic Mapper Multispectral Scanner data as a tool for monitoring water quality (including chlorophyll *a*) and for studying hydrodynamic/biological features of estuaries. However, routine application of the method is not realistic until the significance of potential problems has been resolved. For example,

(1) problems with bottom reflectance or reflectance from exposed mudflats, particularly where chlorophyll concentrations are high in sediments. This is true for northern San Francisco Bay (Thompson et al., 1981), and

the predicted high chlorophyll values around the perimeter of Suisun Bay (Figure 8) may be invalid because of this source of error;

(2) problems with tidal currents--the tidal excursion along northern San Francisco Bay is about 10 km, and water parcels are advected rapidly during the course of sampling from boats. Therefore, care must be taken to ensure simultaneous collection of surface truth and remotely-sensed data, particularly in waters with strong tidal currents;

(3) the success of using MSS data for defining chlorophyll distributions in this study may, in part, result from the relatively homogeneous phytoplankton community composition in the study area. When analogous studies are extended throughout San Francisco Bay (or other estuaries), where phytoplankton community composition (and, perhaps, spectral reflectance properties of algae) may vary spatially, simple empirical models may be less successful. Models may have to be developed for local conditions determined from observation of annual shifts in algal community composition;

(4) we do know from this study that the "best fitting" model and parameter values are somewhat conservative over short (hourly) time scales associated with a tidal cycle. But it has yet to be determined how applicable this model formulation and coefficient values

will be over longer (seasonal) time scales when salinity, turbidity, phytoplankton biomass and their physiological conditions change;

(5) without any measurements of upwelling and downwelling irradiance at the water surface correction for atmospheric influence was not possible in this study. With such premeditated measurements, however, predictions may become more consistently accurate and the model parameters stable (i.e., conservative).

CONCLUSIONS

The results of this investigation indicate:

(1) The Thematic Mapper (TM) aboard Landsats may provide repetitive coverage of this estuary in the wavelength regions applicable to predicting chlorophyll *a* concentration. Band transformations of TM data that correspond to Daedalus 1260 Channels 3 minus 10 and ratio of 7 to 8 are TM Channel 1 minus 5 (.45 to .52 μm - 1.55 to 1.65 μm) and ratio of Channels 3 (.63 to .69 μm) to 4 (.76 to .90 μm), respectively.

(2) Surface concentrations of chlorophyll *a* can be predicted utilizing information in the visible and near infrared wavelength regions of a Daedalus 1260 MSS regardless of tidal stage. The spectral resolution of this scanner was extremely useful in recording wavelength regions influenced primarily by chlorophyll *a*. At the same time, the spatial resolution of this scanner increases the capability of detecting more detailed local variations in surface chlorophyll *a* concentrations as compared to the Landsat MSS system.

(3) In this investigation, model coefficients were similar but not conservative from the morning to the afternoon. Atmospheric correction of data based on surface measured upwelling and downwelling irradiance at various sites during data collection would allow calibration of solar input from morning to afternoon and could possibly contribute to coefficient standardization.

(4) All regression models explained a significant portion of the variability of the measured surface concentration of chlorophyll *a*. Standard errors of the regression of continuous fluorometric surface traces vs. acetone-extracted laboratory measures of chlorophyll *a* are similar to standard errors predicted using remote sensing techniques. Larger sample sizes will be necessary to verify functional models.

(5) Further investigation is necessary to confirm the applicability of the model for different times of year and in different regions of San Francisco Bay. Different models may be needed to predict surface chlorophyll *a* concentrations at different times of year or for a much different part of the bay (i.e., south San Francisco Bay) where phytoplankton species and dynamics differ considerably from the study area. Present knowledge of the actual temporal and spatial variations in phytoplankton dynamics is essential input in developing a tailored remote sensing system capable of monitoring conditions for a local geographic region.

REFERENCES

Anderson, H. M. and A. J. Horne. 1975. Remote sensing of water quality in reservoirs and lakes in semi arid climates. SERL Report No. 75-1. Univ. of CA, Berkeley. NASA Grant #NSG-2003, p. 132.

Arthur, J. F. and M. D. Ball. 1978. The significance of the entrapment zone location to the phytoplankton standing crop in the San Francisco Bay-Delta Estuary. Water and Power Resource Service, USDI, Sacramento, California.

Arthur, J. F. and M. D. Ball. 1979. Factors influencing the entrapment of suspended material in the San Francisco Bay estuarine system. Proc., San Francisco Bay: The Urbanized Estuary, edited by T. J. Conomos (American Association for the Advancement of Science), pp. 143-175.

Arvesen, J. C., J. P. Millard, and E. C. Weaver. 1973. Remote sensing of chlorophyll and temperature in marine and fresh waters. Astronaut Acta 18:229-239.

Ball, M.D. and J. F. Arthur. 1979. Planktonic chlorophyll dynamics in the northern San Francisco Bay and Delta. Proc., San Francisco Bay: The Urbanized Estuary, edited by T. J. Conomos (American Association for the Advancement of Science), pp. 265-287.

Bowker, D. E., C. A. Hardesty, and D. J. Jobson. 1983. Remote sensing of sediment and chlorophyll with the test-bed aircraft multispectral scanner. NASA Tech. Mem. TM:85490, Washington, D.C., pp. 1-23.

Bressette, W. E. and D. E. Lear, Jr. 1973. The use of near-infrared reflected sunlight for biodegradable pollution monitoring. EPA 2nd Env. Quality Sensors Conf., Las Vegas, NV.

Bristow, M. F., B. Bundy, R. Furtek, and J. Baker. 1979. Airborne laser fluorosensing of surface water chlorophyll a. Report EPA-600/4-79-048, EPA, Las Vegas.

Cambell, J. W. and J. P. Thomas. 1981. Chesapeake Bay Plume Study: Superflux 1980. Proc. NASA Conf. 2188, Washington, D.C., pp. 1-515.

Clark, D. K., E. T. Baker, and A. E. Strong. 1980a. Upwelled spectral radiance distribution in relation to particulate matter in sea water. Boundary-Layer Meteorology, 18, pp. 287-298.

Clark, D. K., J. L. Mueller, and W. A. Hovis. 1980b. Phytoplankton pigments from the Nimbus-8 Coastal Zone Color Scanner: comparisons with surface measurements. Science, 210, pp. 63-66.

Clarke, G. L., G. C. Ewing, and C. J. Lorensen. 1970. Spectra of backscattered light from the sea obtained from aircraft as a measure of chlorophyll concentration. Science 67, pp. 119-1121.

Cloern, J. E. 1979. Phytoplankton ecology of the San Francisco Bay system: the status of our current understanding. Proc., San Francisco Bay: The Urbanized Estuary, edited by T. J. Conomos (American Association for the Advancement of Science), pp. 247-265.

Cloern, J. E. and R. T. Cheng. 1981. Simulation model of Skeletonema costatum population dynamics in northern San Francisco Bay, California. Estuarine and Coastal Shelf Science 12:83-100.

Cloern, J. E., A. E. Alpine, B. E. Cole, R. L. J. Wong, J. F. Arthur, and M. D. Ball. 1983. River discharge controls phytoplankton dynamics in the northern San Francisco Bay estuary. Estuarine and Coastal Shelf Science 16:415-429.

Conomos, T. J. and D. H. Peterson. 1977. Suspended-particle transport and circulation in San Francisco Bay: an overview. In M. Wiley (ed.), Estuarine Processes, Vol. 2. Academic Press, New York, pp. 82-97.

Conomos, T. J. 1979. Properties and circulation of San Francisco Bay waters. Proc., San Francisco Bay: The Urbanized Estuary, edited by T. J. Conomos (American Association for the Advancement of Science), pp. 47-84.

Duntley, S. Q., R. W. Austin, W. H. Wilson, C. F. Edgerton, and S. E. McRan. 1974. Ocean color analysis, final report. Naval Res. Lab. Contract: N00014-69-A-0200-6033 and Nat'l.Ocean. and Atm. Admin. Grant No. 04-3-157-64, Scripps Inst. of Ocean., Ref. 74-10.

Farmer, F. H., O. Jarrett, Jr., and C. A. Brown, Jr. 1983. Visible Absorbance Spectra: A basis for in situ and passive remote sensing of phytoplankton concentration and community concentration. NASA Tech. Paper TP-2094. Washington, D.C., pp. 1-32.

Gordon, H. R. and D. K. Clark. 1980. Atmospheric effects in remote sensing of phytoplankton pigments. Boundary-Layer Meteorology, 18, pp. 299-313.

Gower, J. F. R. and G. A. Borstad. 1981. Use of the in-vivo fluorescence line at 685 nm for remote sensing surveys of surface chlorophyll a. In Oceanography from Space, edited by J. F. R. Gower (New York; Plenum), pp. 329-338.

Grew, G. W. 1981. Real-Time Test of MOCS Algorithm During Superflux 1980 in Chesapeake Bay Plume Study: Superflux 1980. J. W. Cambell and J. P. Thomas (eds.), Proc. NASA Conf. 2188, Washington, D.C., pp. 301-322.

Hoge, F. E. and R. N. Swift. 1981. Airborne spectroscopic detection of laser-induced water raman backscatter and fluorescence from chlorophyll a, and other naturally occurring pigments. Applied Optics 20 (18):3197-3205.

Johnson, R. W. 1978. Mapping of chlorophyll a distribution in coastal zones. Photogram. Engr. and Remote Sensing, 44, No. 5, pp. 617-626.

Johnson, R. W., G. S. Bahn, and J. P. Thomas. 1981. Synoptic thermal and oceanographic parameter distributions in the New York Bight Apex. Photogram. Eng. and Remote Sensing 48 (11):1593-1598.

Khorram, S. 1981a. Use of Ocean Color Scanner data in water quality mapping. Photogram. Engr. and Remote Sensing, 47, pp. 667-676.

Khorram, S. 1981b. Water quality mapping from Landsat digital data. Int. J. Remote Sensing, 2, pp. 145-153.

Kim, H. H., C. R. McClain, and L.R. Blaine. 1980. Ocean chlorophyll studies from a U-2 aircraft platform. J. of Geophysical Research, 85 (C7):3892-3990.

Meade, R. H. 1972. Transport and deposition of sediments in estuaries. Mem. Geol. Soc. Am., 133, p. 91.

Morel, A. and L. Prieur. 1977. Analysis of variations in ocean color. Limnology and Oceanography, 22, pp. 709-733.

Munday, J. C. and P. L. Zubkoff. 1981. Remote sensing of dinoflagellate blooms in a turbid estuary. Photogram. Eng. and Remote Sensing 47(4):523-531.

Neville, R. A. and J. F. R. Gower. 1977. Passive remote sensing of phytoplankton via chlorophyll *a* fluorescence. Journal of Geophysical Research 82:3487.

Peterson, D. H., T. J. Conomos, W. W. Broenkow, and E. P. Scrivani. 1975. Processes controlling the dissolved silica distribution in San Francisco Bay. In L. E. Cronin (ed.), Estuarine Research, Vol. 1, Chemistry and Biology. Academic Press, N. Y., pp. 153-187.

Platt, T. and A. W. Herman. 1983. Remote sensing phytoplankton in the sea: surface-layer chlorophyll as an estimate of water-column chlorophyll *a* primary production. Int. J. Remote Sensing, 4, No. 2, pp. 343-351.

Postma, H. 1967. Sediment transport and sedimentation in the estuarine environments. Estuaries, edited by G. H. Lauff (American Association for the Advancement of Science), 83, pp. 158-179.

Richards, R. A. 1952a. The estimation and characterization of plankton populations by pigment analysis. I. The absorption spectra of some pigments occurring in diatoms, dinoflagellates, and brown algae. J. Mar. Res., II. pp. 147-155.

Richards, R. A. and R.G. Thompson. 1952b. The estimation and characterization of plankton populations by pigment analysis. II. A spectrophotometric method for the estimation of plankton pigments. J. Mar. Res., II. pp. 156-172.

Smith, R. C. and K. S. Baker. 1982. Oceanic chlorophyll concentrations as determined by satellite (Nimbus-7 Coastal Zone Color Scanner). Marine Biol., 66, pp. 269-279.

Strickland, J. D. H. and T. R. Parsons. 1972. A Practical Handbook of Seawater Analysis. Fish. Res. Bd. Canada Bull. 167, 310 pp.

Thompson, J. K., F. H. Nichols, and S. M. Wienke. 1981. Distribution of benthic chlorophyll in San Francisco Bay, California February 1980-February 1981. U.S. Geol. Survey Open-File Report 81-1134.

Uno, S., U. Sugahara, and S. Hayakawa. 1980. Remote sensing of chlorophyll found in bodies of water. Proc., 14th Int. Symposium on Remote Sensing of Environment, 2, ERIM, Ann Arbor, MI, pp. 1147-1157.

Walsh, J. J. 1982. The Marine Resources Experiment Program (MAREX): A report by the Ocean Color Science Working Group,Goddard Space Flight Center, Greenbelt, MD.

Wilson, W. H. and D.A. Kiefer. 1979. Reflectance spectroscopy of marine phytoplankton. Part 2, A simple model of ocean color. Limnology and Oceanography, 24, No. 4,

Yentsch, C. S. 1960. The influence of phytoplankton pigments on the colour of sea water. Deep Sea Res., 7, pp. 1-9.